LAWRENCE
LIVERMORE
NATIONAL
LABORATORY

UCRL-TR-233102

Integration & Co-development of a Geophysical CO2 Monitoring Suite

S. Julio Friedmann

July 26, 2007

This work was performed under the auspices of the U.S. Department of Energy by University of California, Lawrence Livermore National Laboratory under Contract W-7405-Eng-48.

FY06 LDRD Final Report

Integration & Co-development of a Geophysical CO_2 Monitoring Suite

LDRD Project Tracking Code: 05-ERD-054

S. Julio Friedmann, Principal Investigator

Abelardo Ramirez, Kathleen Dyer, William Foxall, Jeff Wagoner, co-authors

Abstract

Carbon capture and sequestration (CCS) has emerged as a key technology for dramatic short-term reduction in greenhouse gas emissions in particular from large stationary. A key challenge in this arena is the monitoring and verification (M&V) of CO2 plumes in the deep subsurface. Towards that end, we have developed a tool that can simultaneously invert multiple sub-surface data sets to constrain the location, geometry, and saturation of subsurface CO2 plumes. We have focused on a suite of unconventional geophysical approaches that measure changes in electrical properties (electrical resistance tomography, electromagnetic induction tomography) and bulk crustal deformation (tilt-meters). We had also used constraints of the geology as rendered in a shared earth model (ShEM) and of the injection (e.g., total injected CO_2).

We describe a stochastic inversion method for mapping subsurface regions where CO_2 saturation is changing. The technique combines prior information with measurements of injected CO_2 volume, reservoir deformation and electrical resistivity. Bayesian inference and a Metropolis simulation algorithm form the basis for this approach. The method can a) jointly reconstruct disparate data types such as surface or subsurface tilt, electrical resistivity, and injected CO_2 volume measurements, b) provide quantitative measures of the result uncertainty, c) identify competing models when the available data are insufficient to definitively identify a single optimal model and d) rank the alternative models based on how well they fit available data.

We present results from general simulations of a hypothetical case derived from a real site. We also apply the technique to a field in Wyoming, where measurements collected during CO_2 injection for enhanced oil recovery serve to illustrate the method's performance. The stochastic inversions provide estimates of the most probable location, shape, volume of the plume and most likely CO_2 saturation. The results suggest that the method can reconstruct data with poor signal to noise ratio and use hard constraints available from many sites and applications. External interest in the approach and method is high, and already commercial and DOE entities have requested technical work using the newly developed methodology for CO_2 monitoring.

Introduction/Background

Carbon capture and sequestration (CCS) has emerged as a key technology for dramatic short-term reduction in greenhouse gas emissions in particular from large stationary. A key challenge in this arena is the monitoring and verification (M&V) of CO_2 plumes in the deep subsurface. Confidence in CO_2 storage is limited by the uncertainty in our subsurface knowledge. Subsurface CO_2 plume movement is often difficult to reconstruct due to uncertainties in reservoir architecture, distribution of porosity and permeability, and our ability to predict multi-phase fluid saturations. Similarly, the presence of heterogeneities and fast paths such as faults or abandoned wells that can create failure modes that might lead to CO_2 leakage and shallow migration. Because natural reservoirs are complex, collection and formal integration of multiple geological, geophysical, and geochemical data sets and models can reduce or constrain key uncertainties and maximize our confidence in long-term CO_2 storage.

We have developed a stochastic computational tool to more realistically render CO_2 plume models using multiple geological and geophysical techniques. Importantly, the approach formally and quantitatively integrates available data and provides a strict measure of probability and uncertainty in the plume models. The method will characterize solution uncertainties whether they stem from unknown reservoir properties, measurement error, or poor sensitivity of geophysical techniques.

The rendering of plume geometry and character is highly robust, and new or existing data can often rapidly test predictions of the stochastic tool.

Base Methodology

Our reconstruction method uses Bayesian inference, a probabilistic approach that combines observed data, geophysical forward models, and prior knowledge to compute models of the subsurface CO_2 plumes. Joint reconstruction of the data results in plume models that are consistent with all available data. The result is a distribution of likely plume models. The method uses a Markov Chain Monte Carlo (MCMC) technique to sample the space of possible plume models, including the shape, location and CO_2 content of the plume. MCMC is a proven technique that uses a random-walk type procedure to sample possible outcomes given all available data. A detailed description of the application of the MCMC approach to plume reconstruction is found in Ramirez et al. [1]. Importantly, the basic approach was developed in a prior LDRD-SI proposal as described in Aines et al. [2]

This approach is useful for a variety of subsurface problems such as geophysical inversion, data fusion, and reservoir fluid flow monitoring (water floods, steam injection, CO_2 floods). A key advantage of the approach is that it explicitly treats the non-uniqueness inherent in geophysical inversion. Alternative plume models are identified and then ranked based on how well they fit the data. It can incorporate disparate data types like structural geology maps identifying permeable layers and fracture zones, measurements of the injected CO_2 volume, reservoir deformation data, cross-borehole

electrical resistivity, production data, geophysical logs, temperature measurements, tracer measurements, and gravity data.

Figure 1 schematically illustrates the data processing approach. The box labeled “Propose model” generates random plume models that honor prior knowledge. In our implementation, the following prior data are used: a) reservoir models (i.e., plumes are more likely to be located within permeable regions), b) the plume consists of a region of changing CO_2 saturation embedded within an otherwise unchanging volume, c) the changing region is composed of sub-regions that either overlap or are near each other, and, d) the CO_2 saturation value is in the range 0 – 1.0. The box labeled *Stage 1* in Figure 2 indicates that the proposed plume model is used to predict reservoir deformation and that the predicted and observed deformation data are compared. The “MCMC Bayesian Comparison” box uses the Metropolis algorithm, Metropolis et al. [3], a randomized decision rule to accept or reject the proposed plume models according to their consistency with the observed data. This comparison always involves the current proposal and the last proposal that was deemed acceptable. If the current proposal fits the data better than the last accepted proposal, it is always accepted, and is passed to the box labeled *Stage 2* where a different type of data is considered, e.g., electrical resistivity. If *Stage 2* accepts the proposal using similar criteria as in *Stage 1*, the proposal has been determined to be consistent with all available data and becomes part of the distribution of accepted models. If the proposal is rejected by either *Stage 1* or *Stage 2*, the current proposal is discarded, a new proposal is randomly generated and the process repeats. Mosegard and Tarantola [4] originally described this staged reconstruction approach.

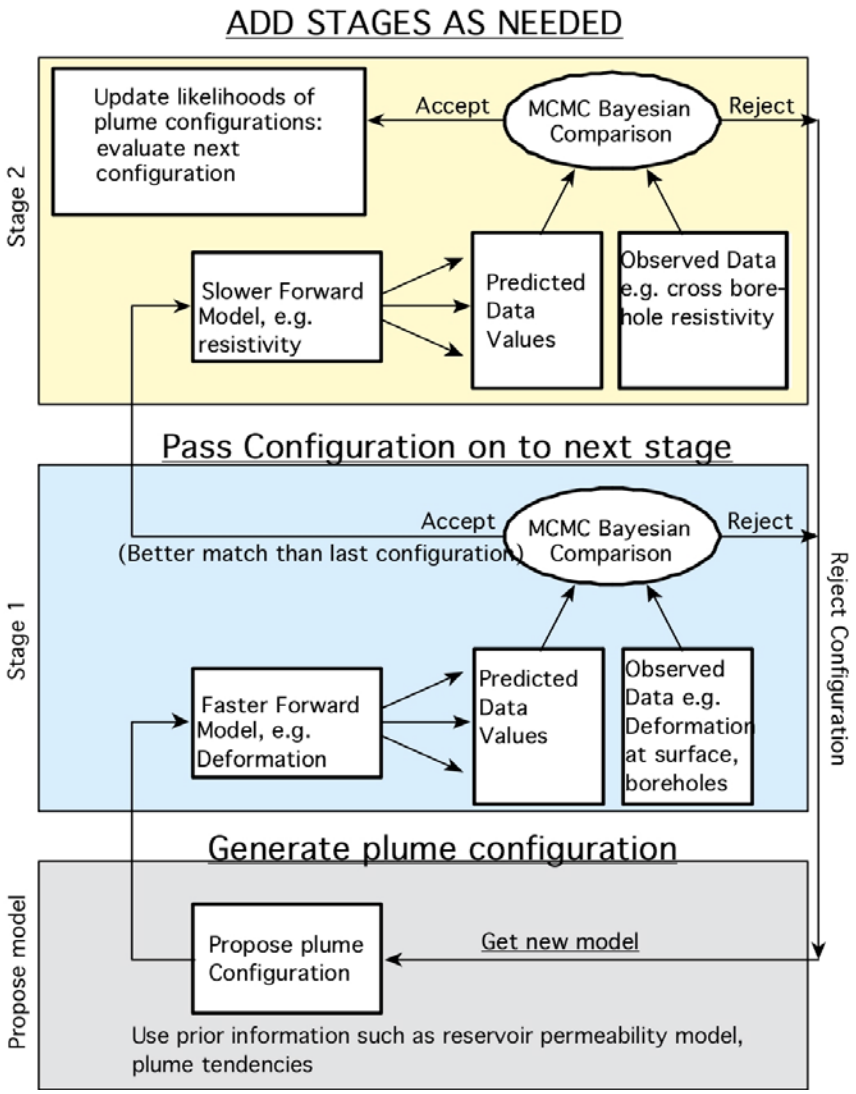

Figure 1 shows a schematic diagram that outlines the MCMC stochastic inversion approach.

Most geophysical inversions are substantially under-determined, ill-posed and non-unique. Thus, the search for a solution that is unique and possesses a high degree of confidence is usually impossible. We believe that it is wise to use inversion methods that consider this non-uniqueness explicitly. The MCMC we describe automatically identifies alternative models and ranks them according to how well they fit the data thereby directly addressing the non-uniqueness problem.

Research Activities

The research effort fell into four general categories:

- Preparation of the Shared Earth Model (ShEM)
- Development of the base sampler, including the random walker
- Development of new algorithms for use in the Stochastic Engine

- Execution of simulations to validate methodology and result interpretation

The final category is discussed in the next section, Results/Technical Outcomes. The first three are discussed below.

Construction of a Shared Earth Model (ShEM)

The Shared Earth Model (ShEM) was the common geoscience data base that served to initialize the stochastic inversion. We began with the Teapot Dome oil-field, which was a readily available public-domain geologic data set. In doing so, we were able to validate our ability to load and manage complex geologic data sets into EarthVision and to transfer those representations into the stochastic engine. The base models used in the simulations was a highly simplified version of the representative geology from this ShEM.

The Teapot Dome Field lies along the southeastern portion of the larger Salt Creek anticline in eastern Wyoming. A framework 3D geologic model was generated using data from a number of sources (figure 2), including RMOTC (DOE), McCutcheon Energy Company, and the Web. The model was developed in UTM coordinates (NAD 27, Zone 13), with a range of 399000-406500E 4788000-4800000 N; the depth ranges from an elevation of 4000 to -3500m below sea level. Stratigraphic data for 28 formations were made available to LLNL and 22 of these surfaces were included in the model. From youngest to oldest, the stratigraphy ranges from the Cretaceous Fox Hills Sandstone to the Precambrian basement rocks. Structural contour grids of these surfaces were generated not only from tags in boreholes, but also from surface exposures. There are 1694 boreholes in this field and many of these holes provided stratigraphic information (figure 3). All boreholes are assumed to be vertical for this version of the model. The upper surface of the model is a topographic grid constructed from 30M DEM files downloaded from the Web. Along with the stratigraphic tops from the boreholes, several horizons were gridded using the excellent 3D seismic data available for the field. Unfortunately, all but one surface (structural top of the basement) were provided to LLNL in a time structure format, which is not compatible with this depth model (figure 4). These surfaces need to be converted to depth (m) before they can be incorporated into the model.

Numerous faults cut through the Teapot Dome Field and some of these faults are included in the geologic model. These data were provided to the project by the McCutcheon Energy Company. Seven faults are included in the current version of the model. Three of the faults are reverse faults, occurring in the basement, but also possibly propagating up into the younger formations. Four normal faults were also modeled. All of the faults are modeled as 2D grids that cut through the formation surfaces. There are many more structures that are visible in the 3D seismic data, but unfortunately these data are only in a time format. These data need to be converted to depth before they can be included in the framework model. This is an important issue, because there are numerous faults in the field and the complex relationships between these structures can only be defined by the quality seismic data.

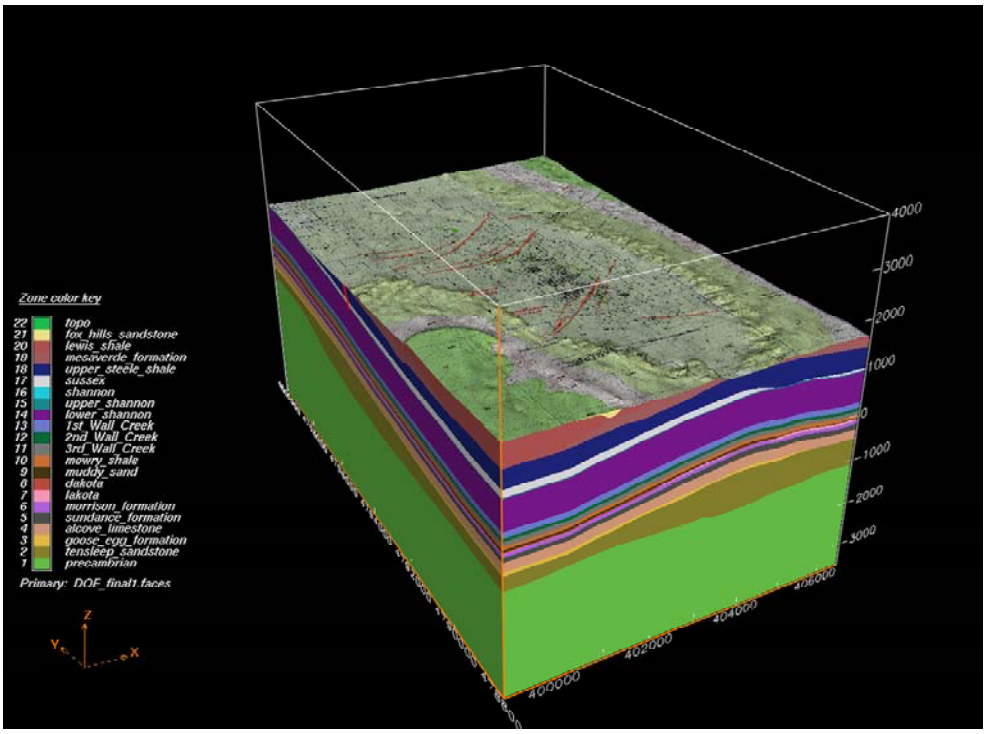

Figure 2. The full static geomodel of Teapot Dome that serves as the ShEM basis. A geo-referenced geologic map draped over the surface. The different horizons represent individual geological layers in the site stratigraphy. Note the locations of the faults projected to the surface (red lines).

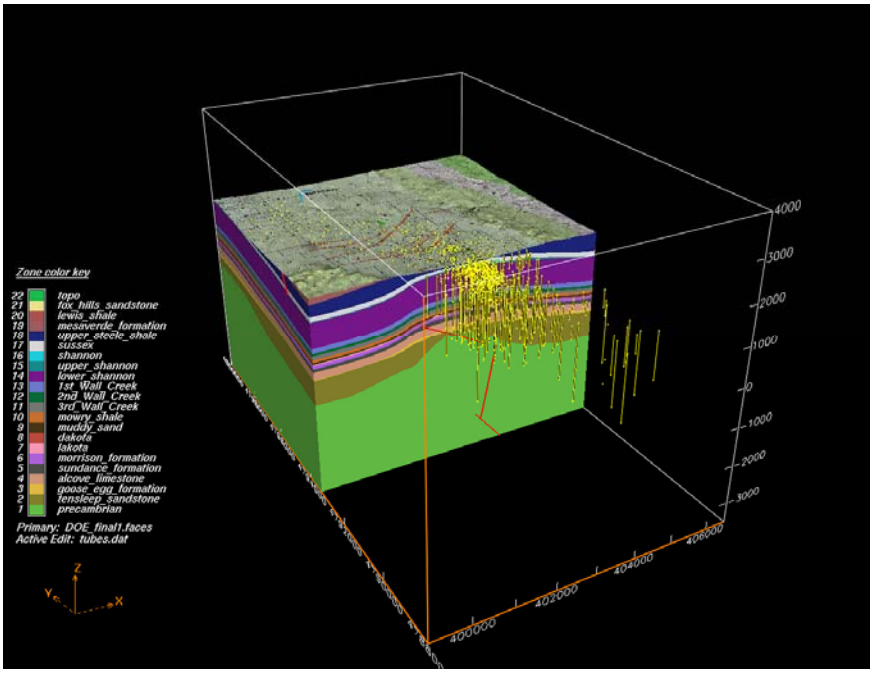

Figure 3: Cut-away view of the same static geomodel. The position, locations, and depths of many boreholes can be seen (yellow). This view also cuts through the center of the anticline and provides a better view of the folding and faults at depth (in red)

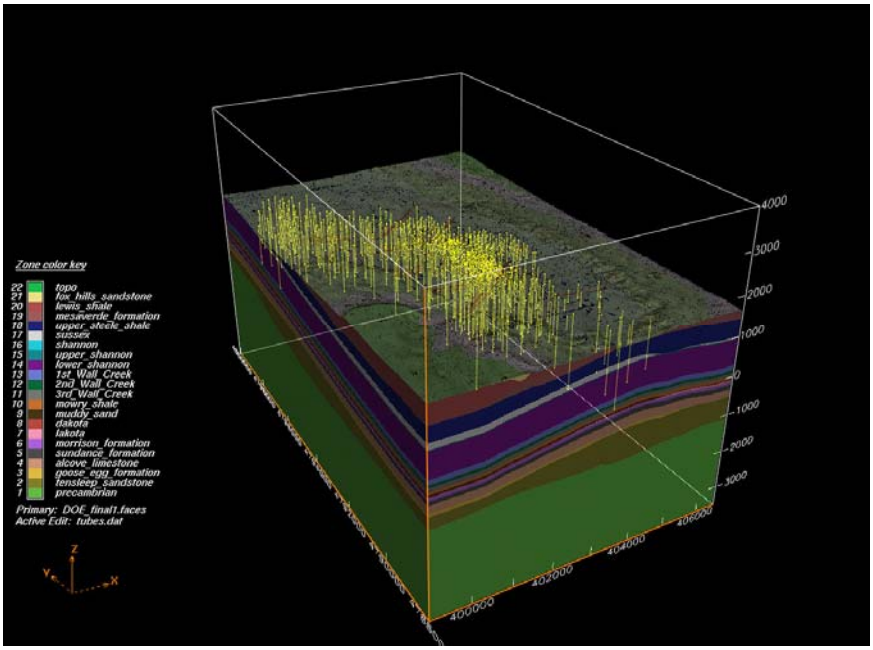

Figure 4: The same view as Figure 2, except that the formations are transparent, allowing a view of the boreholes.

Development of the base sampler

The stochastic engine allows for the initial distribution of CO_2 to be modified by a number of means. For example, it is possible to distribute CO_2 using a multiphase flow simulator and varying the initial model geology. However, while some flow simulation approaches are computationally cheap (e.g., streamline simulators), most are expensive. They are also highly sensitive to the initial conditions of the flow model, which in many CO_2 sequestration applications may not be well known enough to sensibly vary the base sampler.

As such, we developed a method to vary the base representation of a CO_2 plume without running flow simulations explicitly. This approach randomly alters the distribution of CO_2 parameters such as location or saturation. It does so according to user input parameters associated with knowledge of the reservoir. In doing so, it allows CO2 to enter into all units and formation, however does so by applying probabilities of entry as a function of rock properties such as permeability (figure 5). In these cases, the CO_2 retains the same center of mass, but otherwise varies in geometry and saturation. Any configuration of CO_2 is possible; however, users may define aspects of the plume based on CO_2 physics. For example, it is known that in the subsurface CO_2 does not segregate into many separate discrete and discontinuous units, but rather remains coherent. In many simulation runs described below, the user constrained the number of possible separate “bubbles” to be no more than 10, thereby honoring the Co2 phenomenology without being unduly prescriptive.

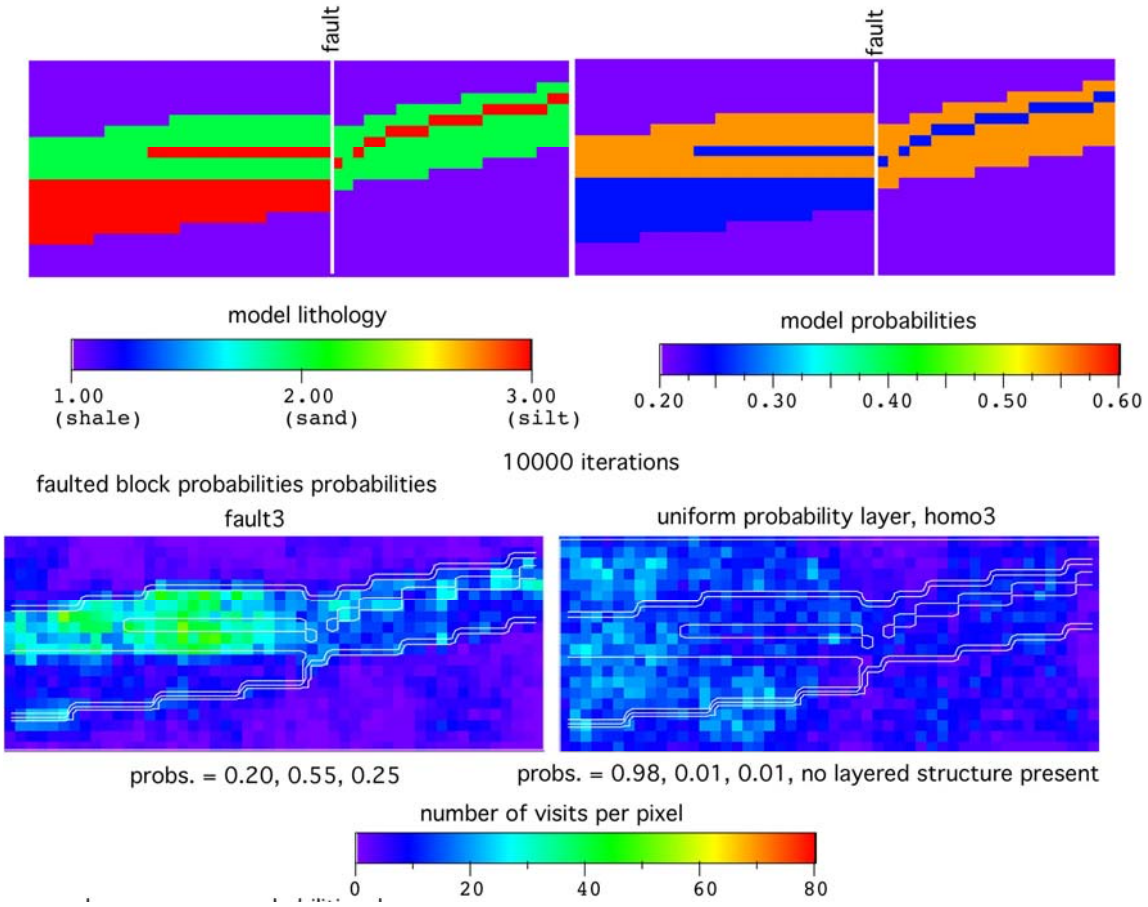

Figure 5. Simple 2-D faulted reservoir model to illustrate random-walker. The fault is considered non-transmissive. Top: Simple schematic showing the base sampling strategy. Model lithologies are derived from the ShEM and allowed to vary between iterations if desired. Within each iteration, CO_2 is allowed to enter lithologies by some probability as a function of lithology. Bottom: Examples of base sample plumes generated with differing probabilities of CO_2 migration by lithology (left) versus uniform probabilities (right).

Figure 6 shows a three-dimensional example that illustrates the random walk approach. Here, The purple region in the 2D images represent a buffer zone with 0 probability, put in to insure good behavior near the edges of the domain for this run (i.e. given that the walker controls the center of mass, the anomaly surrounds this point in space. Near the edges, some pieces of the anomaly could fall outside of the domain, thereby creating problems. The buffer zone prevents this problem). In the 3D space, the initial CO2 distribution is shown on the far left, and allowed to move through the volume with a random walk (while gravitational forces are not acting in this volume, future simulations ran with gravity on). After many iterations, the Co2 preferrentially collected in the permeable strata, yet also visited all strata as part of a probability matrix. These non-zero likelihood solutions are extremely important for proper sampling of probability space and stabilization of the stochastic inversion.

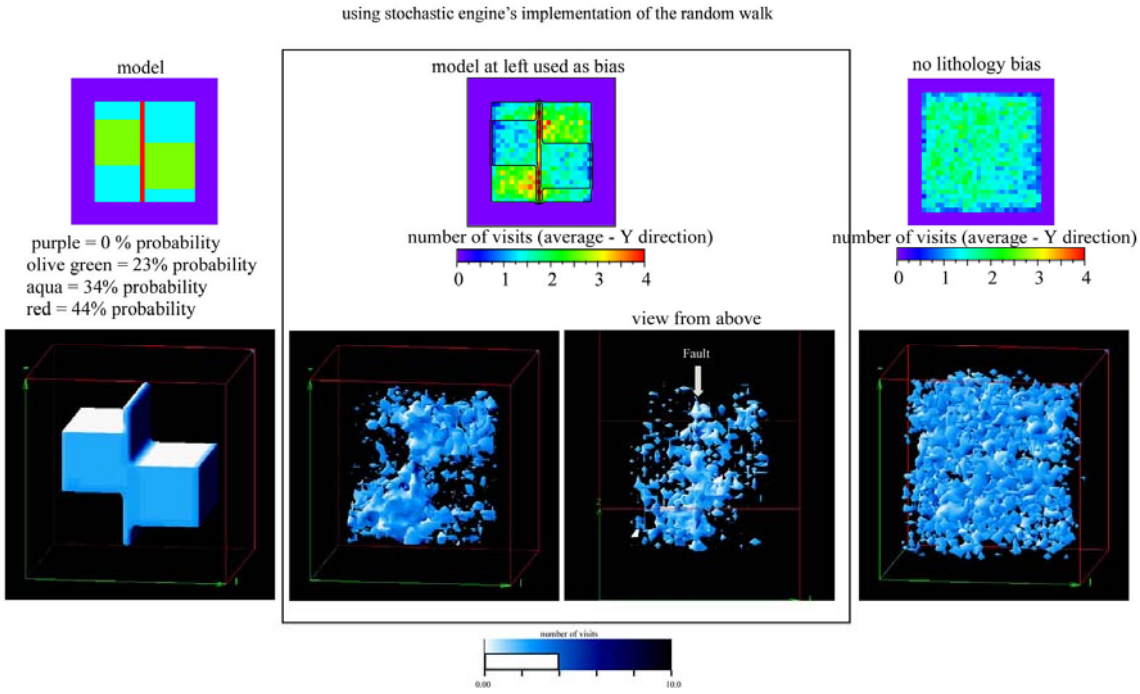

Figure 6: The stochastic engine's implementation of the random-walk sampler. Note the high density of CO_2 along the transmissive fault and preferential entry into permeable strata.

Development of new input algorithms and forward models

At the beginning of the LDRD project, the stochastic engine was not configured to invert geophysical signatures for CO2. We initially proposed to develop inversion algorithms using forward solvers for changes in electrical resistivity, electromagnetic induction, bulk crustal deformation, and microseismic acoustic emissions. After beginning the LDRD, we recognized that microseismic inversion was prohibitively expensive and complex and would require additional work beyond the scope of the initial LDRD proposal. As a result, this effort was removed during the renewal request.

Three forward solvers were added to the stochastic engine. These were for electrical resistance tomography (ERT), tilt-meter data (herein referred to as tilt), and electromagnetic induction tomography (EMIT). All these approaches entered the engine and were normalized so as to share and compare data with each other, the ShEM, and the base sampler. In addition, two different approaches to ERT inversion were developed and added to the engine. The first uses only long-electrodes as the source of the data (LEERT). The second uses only a spaced vertical electrode array (VERA). As such, methodologies for four different geophysical data streams are now the core of the inversion capability.

In running the applications, the team discovered that it was possible to use additional parameters as either prior or new information to constrain the inversion. These include pH, temperature, pressure, CO_2 injected volume, produced volumes, and injected brine volumes. The team only developed algorithms for CO_2 injected volume, but have plans to continue developing algorithms for the additional parameters in future applications.

The forward and inverse models were run on LC's MCR platform. Ultimately, stabilization required less than 12 hours using a relatively small number of processors. For example, the Salt Creek inversion presented below required less than nine hours and only 56 processors to stabilize a real-world two-stage inversion of a 3D heterogeneous model. Based on these results, the team is confident that larger and more complicated inversions would stabilize as well, even with complex data sets and complex rock geometries.

Results/Technical Outcome

Overall, the research proved successful. The team was able to execute multi-stage inversions around simulated CO_2 plumes and real field cases. In all cases, families of results were subdivided into like solutions and the likeliest plume geometries and saturations calculated. The calculation explicitly yielded the probability (likelihood) of each solution set and provided information that could be used to test between alternate models or recommend additional data needed to provide greater uniqueness.

A key to successful use of the stochastic engine is the staging order of different data streams to provide the greatest information in a computationally parsimonious manner. This generally involves making the cheapest calculations first. Through testing the algorithms and comparing run times between options, the following staging order emerged for the current set of applications

1. CO_2 injection volume
2. Tilt
3. LEERT
4. VERA
5. EMIT

Each of these is described in greater detail below. As new capabilities are added to the engine, the staging order would change to reflect the robustness of the calculations and their cost. Unfortunately, technical difficulties with MCR cause delays and cost run-ups that prevented formal testing of EMIT stages. We hope to complete this work in future efforts.

Results using simulated data

We have tested the performance of our MCMC staged approach using synthetic and measured field data. In this section we discuss the synthetic data results. Some of the

benefits of the MCMC approach are: its ability to jointly reconstruct disparate data types, identify competing models when the available data are insufficient to definitively identify a single optimal model and, d) rank the alternative models based on how well they fit available data. The results presented below help to illustrate these benefits.
We have chosen geophysical techniques that are likely to be used during injection operations. The methods chosen are cost-effective, non-invasive (requiring no additional boreholes for sensor placement) and are sensitive to the presence of CO_2 in the reservoir. Some of the techniques are sensitive to the subsurface deformations that occur when the reservoir pressure changes due to the injection process. These techniques include surface or subsurface tilt measurements, surface deformations using GPS receivers and INSAR (interferometric synthetic aperture radar on satellite platforms). These measurements are primarily sensitive to the pressure field, volume of CO_2 in the reservoir, and location of the plume.

We have also considered cross-well electrical resistivity measurements using borehole casings as long electrodes. Long electrodes provide a cost-efficient way of injecting electrical current within the reservoir to measure changes in pore fluid resistivity (Daily et al. [5]). The CO_2 displaces native pore water thereby increasing the resistivity locally within the reservoir. The method requires no new wells nor does it affect injection/production operations. It produces data with low signal to noise ratios because only a small fraction of the injected current actually flows through the reservoir. This data is primarily sensitive to the horizontal position and shape of the plume and, to a lesser extent, the amount of CO_2 present.

Figure 7 shows details of the model constructed for this effort. We assume that CO_2 is injected within a 27 m thick reservoir layer located 934 m below the surface. Geophysical measurements are made before and after the CO_2 is injected. The CO_2 injection pressure causes the reservoir layer and overburden to deform. It also causes the pore fluid resistivity to substantially increase. Figures 7 and 8 show the location of electrodes (used for the resistivity surveys) and the tilt-meter locations. Note that the tilt-meter spacing is much broader than the electrode spacing. The broader spacing is needed to capture all the relevant details of the deformation field.

Geophysical inverse problems are typically non-unique and often ill-posed. Prior information is required to stabilize the search for models. We assume the following prior data: a) the CO_2 saturation values are in the range 0.0 – 1.0, b) the plume only penetrates the permeable reservoir layer and not the surrounding impermeable layers, c) the CO_2 saturation values in local areas of the plume are similar, and d) plume consists of individual pieces that tend to be contiguous to at least one other piece.

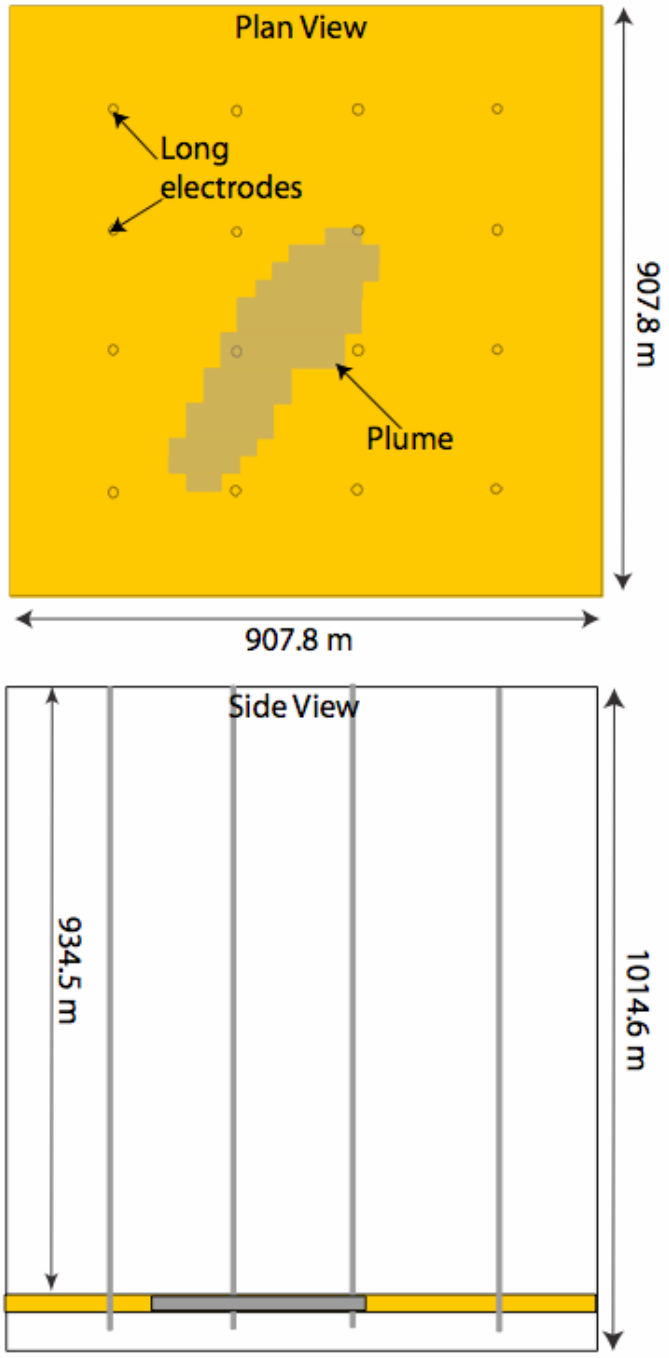

Figure 7 shows plan and side views of the model used to generate the synthetic data. We assume that CO_2 is injected in a 27 m thick reservoir located 934 m below the surface. There are boreholes with metallic casing (indicated by the black circles in the plan view). We assume that geophysical surveys are performed before and after the plume is in place. The side view shows the metallic casings as grey vertical lines that penetrate the reservoir layer shown in orange. The side view also shows the lateral position of the plume within the reservoir layer.

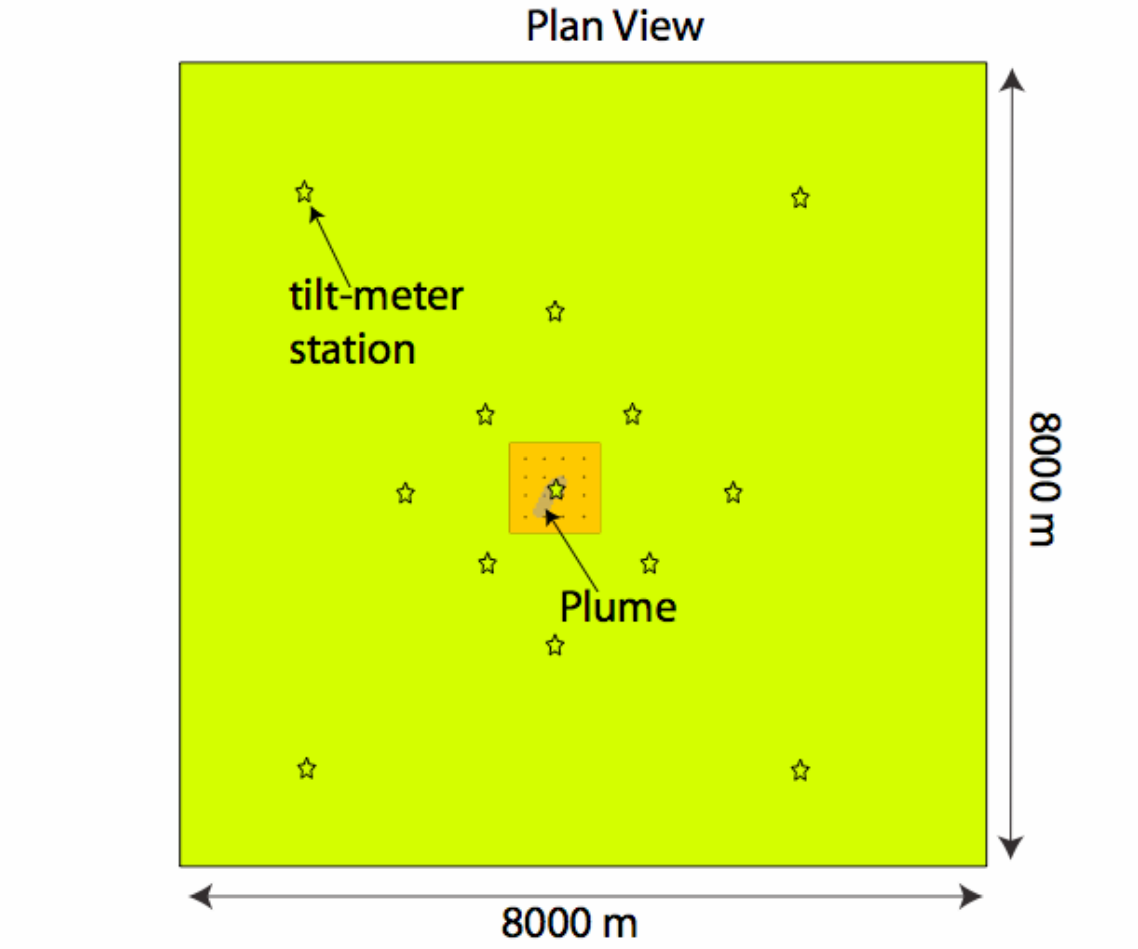

Figure 8 shows a plan view with the locations of the tilt-meter stations (shown as stars). The small orange square near the center is the same as the plan view shown in Figure 1. Note that the tilt-meter spacing is much larger than the long electrode spacing.

After an MCMC run is finished, it is necessary to verify that the accepted models are trustworthy, i.e., provide a statistically valid sample of the unknown posterior distribution (see Ramirez et al. [1] for details). We also need to distill the relevant information from the models in the posterior distribution so that the likely properties of the actual plume model can be identified. We use a clustering technique to extract this insight. We compare all the 3D models in the posterior distribution against each other and automatically group them into clusters of similar models. We then average the models within each cluster. These cluster averages represent competing models that satisfy the available data when the data is insufficient to identify a single “optimal” model. We also compute the probability that a given cluster exhibits properties that are closest to the “true” model under study.

Suppose that the only information collected was the cross-borehole resistivity data and that this data was inverted using our stochastic inversion approach. Figure 9 illustrates the results for this case. We show only a 2D top view of the 3D cluster averages, because the

"true" plume is horizontal and thus, most of the interesting features can be observed in this view. The "true" plume shape and location is indicated by the gray outline; the "true" injected CO_2 volume is 234000 m^3. Note that the top left cluster average is the "best", i.e., it has 53% probability of exhibiting properties that are closest to the "true" model. This means that the members of this cluster are the most consistent with the available resistivity data. Alternative models and their probabilities (24% and 18%) are shown at the top-right and bottom-left of Figure 9; these models are less consistent with the resistivity data. The three cluster averages shown represent 95% of the models in the posterior distribution. Additional clusters were identified but are not shown here for the sake of conciseness and also because their probabilities are quite small. The bottom right model is the average of all models in the posterior distribution. All four images are reasonably close to the "true" model. We believe this mainly reflects the fact because the data used has minimal error compared to real field data. As we will see in the section "Results using field data", the results change considerably when real field data with poor signal to noise is used. This is mainly due to the way electrical currents flow when a resistive anomaly like a CO_2 plume is in its path. The current tends to go around the plume instead of through it, thereby degrading the sensitivity to the CO_2 inside the plume.

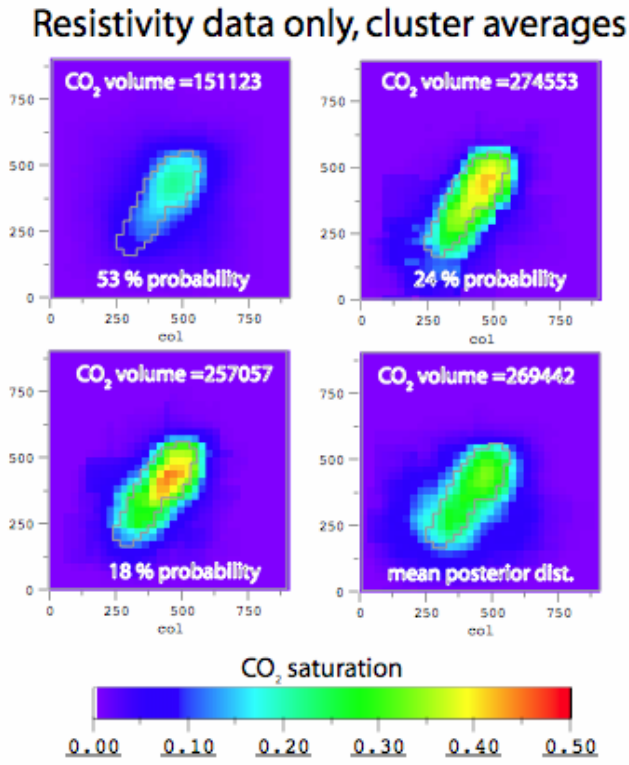

Figure 9 the stochastic inversion results obtained when only the resistivity data are used. We show only a 2D top view of the 3D reconstructed models, models because most of the interesting features can be observed in this view. The "true" plume shape and location is indicated by the gray outline; the "true" volume of CO_2 is 234000 m^3. Thee total amount of CO_2 within the reconstructed plume is indicated.

Note that some of the recovered CO_2 volumes in Figure 9 are substantially different from 234000 m^3.

Let us now consider the case where the resistivity and injected volume data are jointly inverted. The results are shown in Figure 10. When compared to Figure 9, there are slight improvements when in the shape and size of the plume anomaly. As expected, the amount of CO_2 inferred to be in the reconstructed plume models in Figure 10 is closer to the true CO_2 volume of 234000 m^3. When the resistivity data is quite noisy, we expect that the addition of the injected volume data will result in more significant improvements. This improvement will be observed when we discuss results that use real field data in a later section.

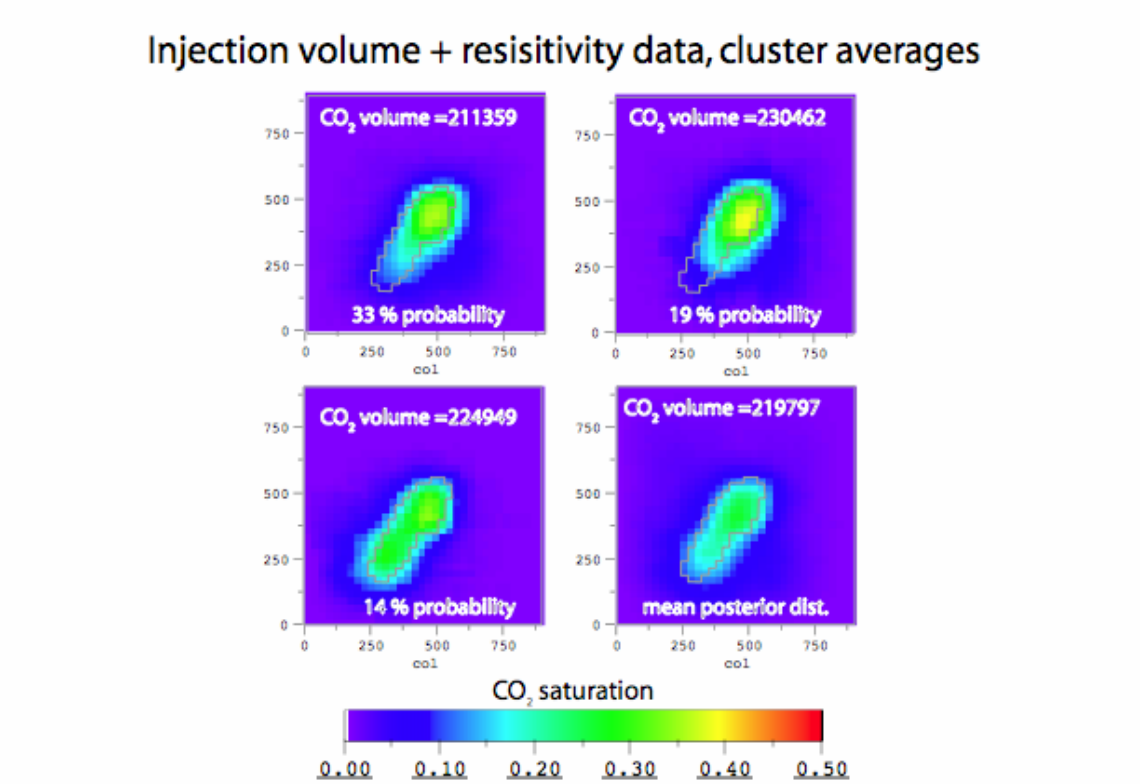

Figure 10 shows the stochastic inversion results obtained when injection volume data and resistivity data are jointly inverted using a staged approach. The "true" plume shape and location is indicated by the gray outline. We also indicate the total amount of CO_2 indicated by the plume.

We now consider the case where deformation data (measured with tilt-meters) are reconstructed. Figure 11 shows the cluster average images for the case where deformation data is used. These reconstructions show circular anomalies located near the plume's center. The amount of CO_2 inferred to be in the reconstructed plume models is quite close to true CO_2 volume of 234000 m^3. This is because the deformation data is very sensitive to the volume of CO_2 present in the reservoir. However, the shape of the

anomaly is not well resolved. In contrast, the resistivity measurements are better able to resolve the plume's shape but do a poorer job of recovering the injected CO_2 volume.

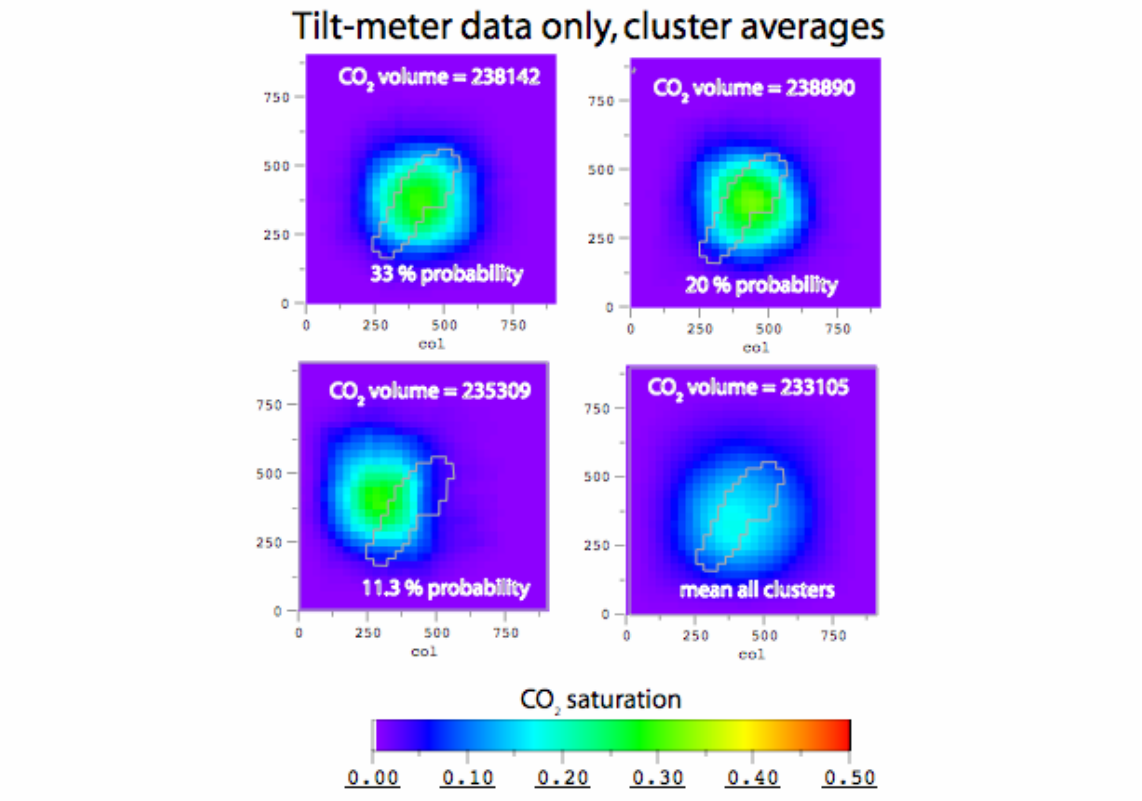

Figure 11 shows the stochastic inversion results obtained when tilt-meter data is inverted. The "true" plume shape and location is indicated by the gray outline. We also indicate the total amount of CO_2 indicated by the plume.

These results suggest that the resistivity and deformation techniques may complement each other well and that jointly inverting these data is advantageous. This hypothesis can be evaluated by examining the results shown in Figure 12. The top and bottom row of images show top views of the cluster average images. The middle row of images shows side views of the cluster averages shown in the first row. We suggest that these cluster averages are closer to the "true" model than any of the results shown in previous figures. The size, location and shape of the plume compare favorably to the "truth". Note that the top two clusters show recovered CO_2 volumes that are within 1.8 and 0.3% of the true volume. In contrast, the recovered CO_2 volumes are within 35 and 17 % of the true volume when only the resistivity data is used. This performance illustrates the value of jointly inverting data sets that are orthogonal, i.e., sample different physical phenomena associated with the presence of CO_2 and have statistically independent errors.

The two most probable clusters in Figure 12 are very similar in shape, location and CO_2 content. Their probabilities (27 and 25 %) are also very similar. In side view, one the images shows most of the mass in the bottom half of the image and the other in the top half. The results imply that the data used is insufficient to discriminate between these two

alternatives. The long electrode resistivity approach does not offer any vertical resolution and the tilt-meter-meter offers only coarse vertical resolution. An analyst evaluating these results would need to consider both alternatives as equally likely.

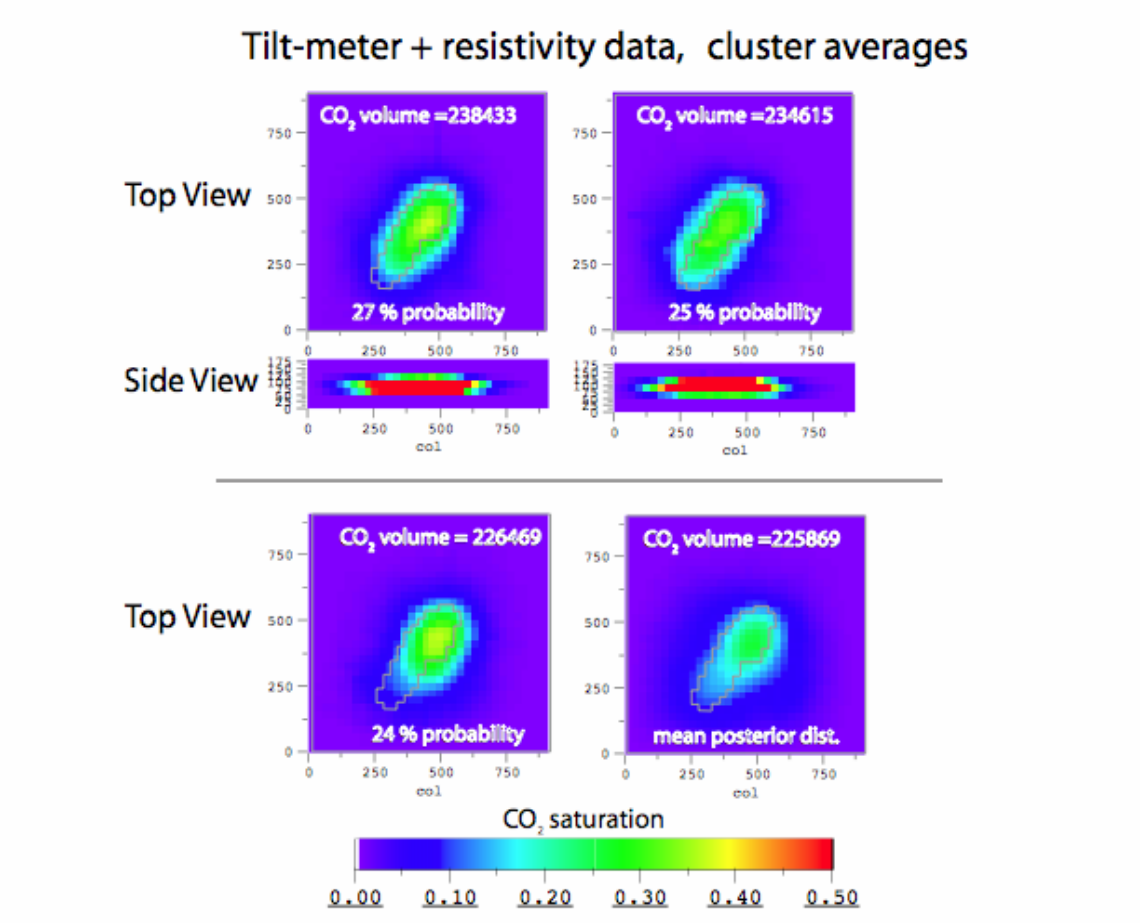

Figure 12 shows the stochastic inversion results obtained when tilt-meter and resistivity data are jointly inverted. The top and bottom row of images show top views of the cluster average images. The middle row of images shows side views of the cluster averages shown in the first row. The "true" plume shape and location is indicated by the gray outline. We also indicate the total amount of CO_2 indicated by the plume.

Sometimes some of the data sets available provide redundant instead of orthogonal information. Consider the results shown in Figure 13 where CO_2 injection volume and tilt-meter data are jointly inverted. Figure 13 can be compared with Figure 11 where only the tilt-meter data is used. The results in these figures are very similar thereby indicating that adding CO_2 injection volume data has not made a significant difference to the results. The tilt-meter data is very sensitive to the volume of CO_2 present in the reservoir and thus, measurements of CO_2 injection volume do not add any new information to the inversion. In real applications, this type of comparison is invaluable because it helps identify the "value-added" by each measurement technique to the final result and helps decision-makers decide whether the costs of a survey are worth the benefit.

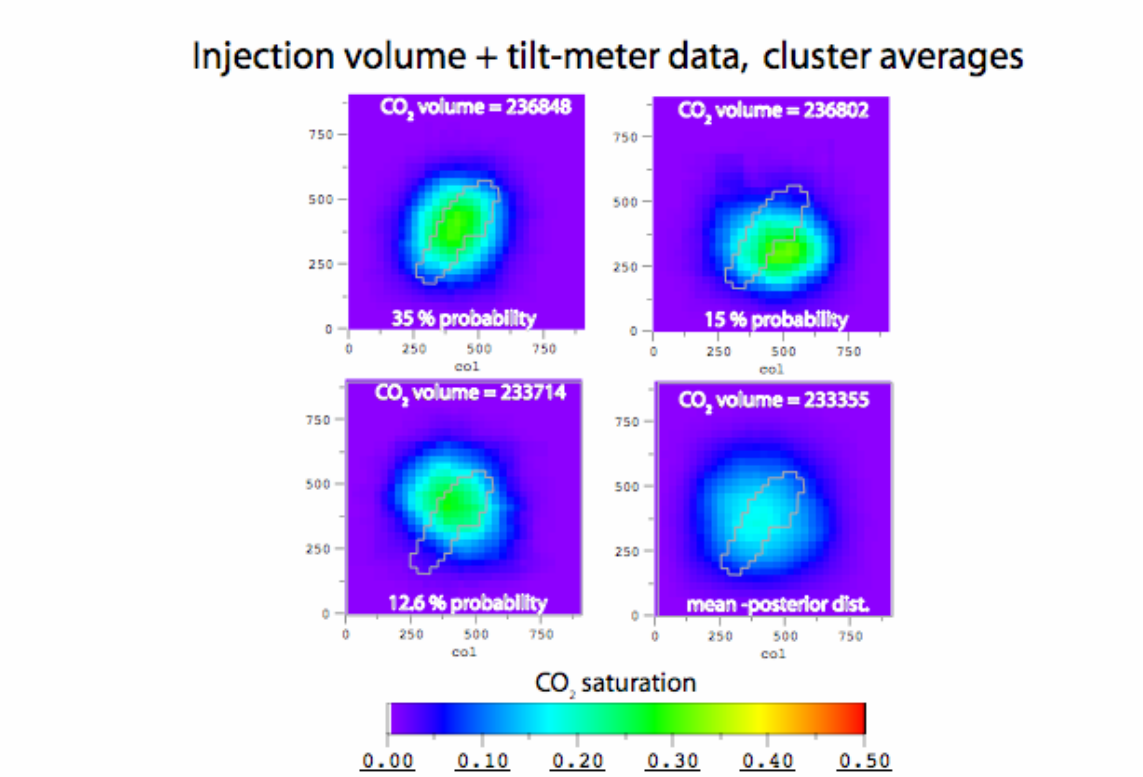

Figure 13 shows the stochastic inversion results obtained when CO_2 injection volume and tilt-meter data are jointly inverted. The "true" plume shape and location is indicated by the gray outline. We also indicate the total amount of CO_2 indicated by the plume.

Results using real field measurements

We also used real field data to test the performance of our approach so that effects of realistic measurement noise and modeling error can be evaluated. We have reconstructed data from a real CO_2 plume injected within a petroleum reservoir. The reservoir lies within the Salt Creek field, located near the southern tip of the Powder River Basin, Wyoming, U.S.A. Figure 14 shows top and side views of the injection site. The block of interest is approximately 0.5 km by 0.5 km by 0.75 km. Seventeen abandoned steel wells were used as long (~710 m) electrodes to conduct cross-well electrical resistivity surveys. At the Salt Creek site, most of the long electrodes only reach to the top of the reservoir thereby reducing the sensitivity to changes within the reservoir. Measurements of injected CO_2 volume were also available.

Geophysical data was collected before and during injection so that the changes caused by the CO_2 could be detected. We first used a well-known, well-behaved, and regularized deterministic inversion algorithm (Morelli and LaBrecque, [6]) to process only the electrical data.

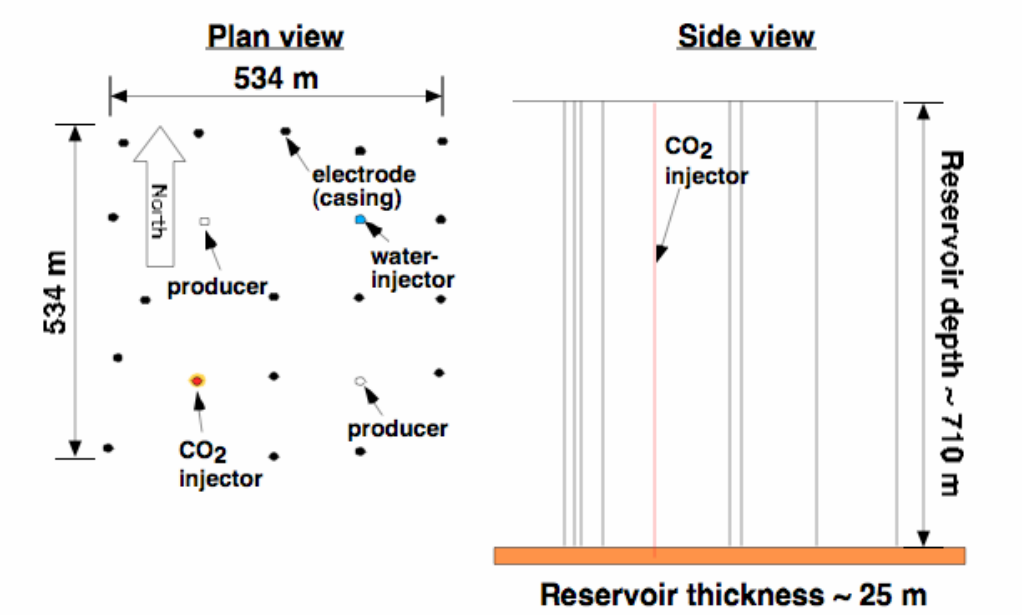

Figure 14 shows plan and side views of the field site located within the Salt Creek field, Wyoming, USA. The red and white circles (left side of the figure) indicate the location of the injection and producing wells. The black circles indicate the location of the long electrodes (metal casings within abandoned wells). The CO2 was injected within a 25 m thick layer located 710 m below the surface.

The deterministic result is shown in Figure 15. We only show a top view of the 3D block because this geophysical technique provides spatially constrained solutions only in horizontal model planes (Daily et al., [1]). Note that most of the tomograph is green, indicating a resistivity ratio (post-injection divided by pre-injection) near 1.0 (i.e., no change). Elsewhere, small changes are scattered throughout the image. We believe this uninformative result is due to the poor signal to noise ratio associated with the long electrode data.

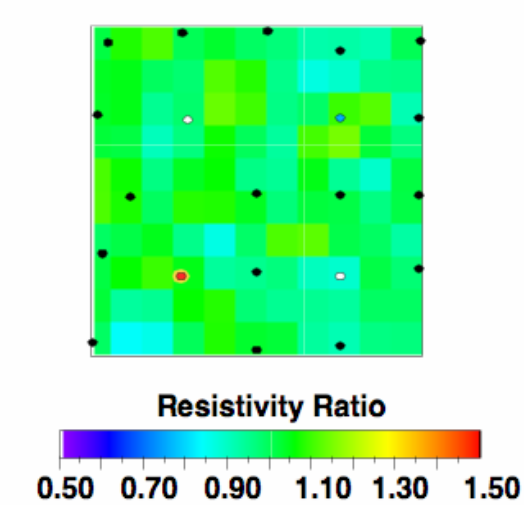

Figure 15. The figure shows the results of a deterministic, time-lapse inversion after approx. 4600 m^3 of CO_2 had been injected). The locations of the injector/producer wells and of the long electrodes are shown for reference.

We also processed the same data electrical data using the MCMC approach. Figure 16 shows the two most likely models found by the stochastic inversion. The model on the left is the most probable result, i.e., the result that is most consistent with all the available data. Synthetic model experiments suggest that such radially symmetric models are indicative of data with a very poor signal to noise ratio.

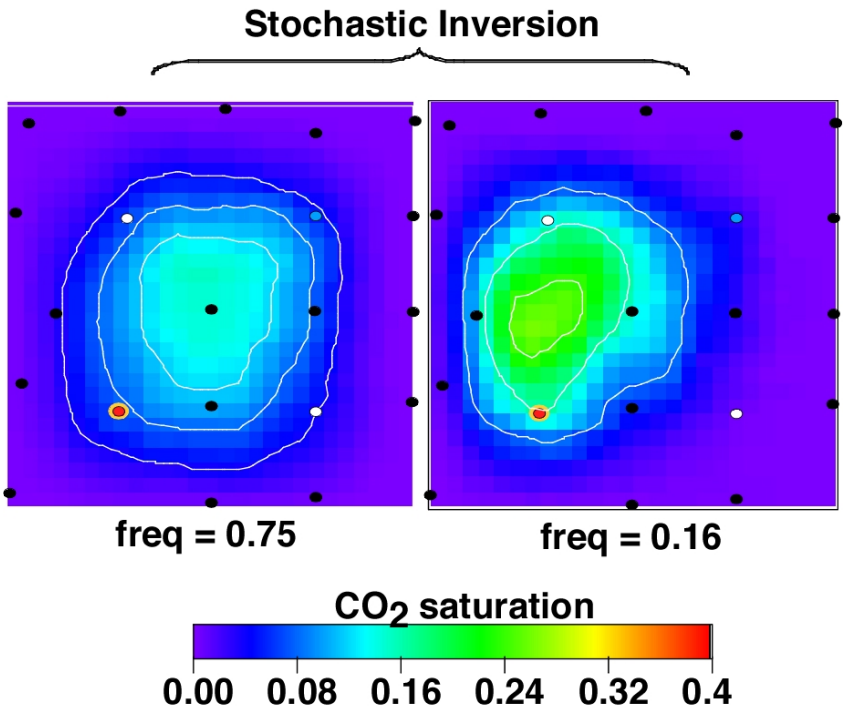

Figure 16 shows the results of a time-lapse stochastic inversion using the MCMC approach after approx. 4600 m^3 of CO_2 had been injected. The left frame shows the "best" model, i.e., the one that is most likely because it is most consistent with the data; the right frame shows the second best model found. The only observations used in this case were the cross-well resistivity data.

The model on the right of Figure 16 is the second most probable result. It shows an anomaly that spans the region between the injection and extraction wells and is more consistent with our expectations of a plume. These results suggest that the data contain a small amount of signal from the CO_2 plume that is nearly overwhelmed by the noise. We decided to jointly invert injected CO_2 volume and resistivity data in order to improve the confidence in the results.

Figure 17 shows the results obtained when the cross-well resistivity and injected CO_2 volume data were jointly reconstructed. The figure shows the most likely plume anomalies (cluster averages) after 4600 and 6300 m^3 had been injected (approximately 2 weeks and 5 weeks after injection started). The left frames in Figures 16 and 17 show the effect of using the injected CO_2 volume; i.e., the radially symmetric anomaly (in Fig. 16) changes to an elongated anomaly (in Fig. 17) that connects the injection and extraction wells. Adding the injected volume data as an additional constraint enhances the effect of

very small resistivity changes caused by the CO_2 in the reservoir. Also note that the probabilities for the images corresponding to 4600 and 6300 m^3 of CO_2 are 78% and 97% (respectively). As expected, confidence in the results improves as the volume of injected CO_2 increases and the measured signals become stronger.

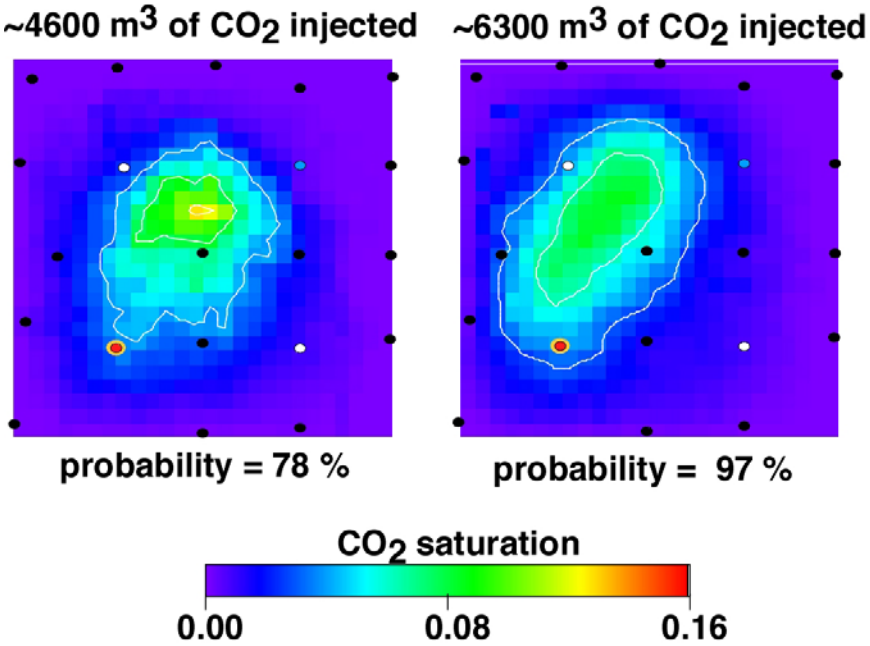

Figure 17 shows the results of two time-lapse stochastic inversions using the MCMC approach after approx. 4600 and 6300 m^3 had been injected. The images show the most likely model found, approximately two and five weeks (left and right frames, respectively) after injection. Note that there is a clear indication of a plume extending from the injection well towards one of the producing wells.

The improvement in rendering of the plume did not involve extensive repeat surveys. Rather, the addition of limited orthogonal data (in this case, injection volume) significantly constrained possible outcomes. Other kinds of constraints (e.g., production data, pressure or temperature data, first breakthrough of CO_2) may also constrain solution space. Our experience with the MCMC approach reveals that new data orthogonal to initial data often improves attribute prediction. It can also help illuminate which data provide the highest value in terms of reducing uncertainty.

Exit Plan

The LDRD exit plans included an aspect of publication and presentation at meetings as well as explicit outreach and contracting with an external organization. We are pleased to report success in both venues.

Regarding external publication, the results of the LDRD project were presented at two flagship international meetings for CO2 sequestration. The first is hosted by the DOE and runs for NETL as an annual meeting [7]. The poster and associated paper received

substantial attention there, as well as at several professional meetings including the annual meeting for Society of Petroleum Engineers. These in turn generated interest in the high-performance computing community and publication in industrial journals [8]. This effort culminated in the eighth annual conference on Greenhouse Gas Technology in Trondheim, Norway, led by the International Energy Agency, with the poster and associated paper appearing as a peer-reviewed publication [9].

The interactions and interest from external parties has been equally strong. As stated explicitly in the initial proposal, we believed that companies would be sufficiently interested to provide data and support for both simulations and field efforts. This has proven to be true. At the end of FY06, LLNL entered into a CRADA with Chevron to use the stochastic engine in a field fluid injection application. Importantly, the choice of geophysical methods proved important – they were most interested in crustal deformation and injection volume since these data were available from their commercial efforts. The team is currently pursuing an additional agreement to add LEERT to the inversion suite.

In addition, other industrial groups have expressed strong interest in the capability developed under this LDRD. BP is considering use of the stochastic inversion capability for CO2 injection operations in the US and abroad, and has agreed to share data to help initialize the project as part of a parallel WFO under consideration. The Weyburn project in Canada has requested a proposal to expand this technique to include seismic and geochemical approaches, and is considering full funding to expand the Lab's capabilities further. Separately, the DOE has begun the solicitation process for large injection projects through their Regional Carbon Sequestration Partnerships. LLNL has received requests from two partnerships for joint inversion using the stochastic engine based on the current results, and is anticipating a third in the coming weeks. Finally, Schlumberger is considering the LDRD results as a basis for a CRADA to commercially develop the inversion suite for the purposes of CO_2 management within its new Carbon Services Company.

Summary

In order to manage CO2 injection, advanced technologies for monitoring and verification will help increase fidelity, reduce uncertainty, and reduce costs. LLNL has developed a geophysical inversion suite which uses the stochastic engine as the central application to invert field CO2 plume measurements for plume geometry and saturation. Having tested this application on synthetic and real data sets, we are confident that this approach can be deployed readily in the field with the current capabilities. The team anticipates expanding this capability further through industrial contracts and DOE-sponsored field tests.

Acknowledgements (if applicable)

This work was performed under the auspices of the U.S. Department of Energy by the Lawrence Livermore National Laboratory under contract W-7405-ENG-48. This work was funded under the LDRD program, and many thanks are given to the program and to

Rokaya Al-Ayat, who administered our program. Thanks to LC for computational resources, and to Doug Rotman who coordinated the LC accounts and interactions. Thanks to Barry Kirkendall for his early work on the project. Thanks to Doug Rotman, Norm Burkhard, and C.K. Chou for helping to support the initial submission of work.

References

[1] Ramirez, A. L., J.J. Nitao, W.G. Hanley, R.D. Aines, R.E. Glaser, S.K. Sengupta, K.M. Dyer, T.L. Hickling, W.D. Daily, 2005, Stochastic Inversion of Electrical Resistivity Changes Using a Markov Chain, Monte Carlo Approach, *Journal of Geophysical Research,* vol 110, no. B2, B02101, doi:10.1029/2004JB003449

[2] Aines R, J. Nitao, R. Newmark, S. Carle, A. Ramirez, D. Harris, J. Johnson, V. Johnson, D. Ermak, G. Sugiyama, W. Hanley, S. Sengupta, W. Daily, R. Glaser, K. Dyer, G. Fogg, Y. Zhang, Z. Yu, and R. Levine, 2002, The Stochastic Engine Initiative: Improving Prediction of Behavior in Geologic Environments We Cannot Directly Observe Lawrence Livermore National Laboratory Report UCRL-ID-148221, 65p.

[3] Metropolis, N., A. Rosenbluth, M. Rosenbluth, A. Teller, and E. Teller, 1953, Equation of state calculations by fast computing machines, *J. Chem. Phys*., 1, no. 6, 1087-1092.

[4] Mosegaard, K., and A. Tarantola, 1995, Monte Carlo sampling of solutions to inverse problems, *Journal of Geophysical Research*, 100, no. B7, 12431-12447.

[5] Daily, W., A. Ramirez, R. Newmark, and K. Masica, 2004, Low-cost reservoir tomographs of electrical resistivities, *The Leading Edge*, 23, no. 5, 472 – 480.

[6] Morelli, G. and D. LaBrecque, 1996, Advances in ERT modeling, *Eur. J. Environ. Eng. Geophys.*, 1, 171-186.

[7] Ramirez, A., Friedmann, S.J., Foxall, W.A., Kirkendall, B., Dyer, K., 2006, Subsurface imaging of CO_2 plumes using multiple data types and Bayesian inference, NETL 5th Annual Conference on Carbon Sequestration, Alexandria, VA, ExchangeMonitor Publications

[8] Friedmann, S.J., 2006, “Big Iron” Linux clusters driving step changes in interpretation, simulation, American Oil and Gas Reporter, v49, p. 80-84

[9] Ramirez, A, Friedmann, S.J., Foxall, W.A., Dyer, K, Kirkendall, B., Aines R., Daily W., 2006, Joint reconstructions of CO2 plumes using a Markov Chain Monte Carlo approach, 8th Greenhouse Gas Technology Conference, Trondheim, Norway, session I3-3